



# Experimental analyses on heat transfer performance of TiO<sub>2</sub>–water nanofluid in double-pipe counter-flow heat exchanger for various flow regimes

R. Subramanian<sup>1</sup> · A. Senthil Kumar<sup>1</sup> · K. Vinayagar<sup>1</sup> · C. Muthusamy<sup>1</sup>

Received: 27 November 2018 / Accepted: 1 October 2019 / Published online: 12 October 2019  
© Akadémiai Kiadó, Budapest, Hungary 2019

## Abstract

Nanofluids are widely used in heat transfer applications. This article presents the effect of heat transfer and pressure drop of the TiO<sub>2</sub>–water nanofluids flowing in a double-tube counter-flow heat exchanger with various flow patterns. In this experimental work, performance of TiO<sub>2</sub>–water nanofluid on heat transfer in three different cases such as laminar, transition and turbulent flow region were analyzed. TiO<sub>2</sub> nanoparticles with average diameters of 20 nm dispersed in water with three volume concentrations of 0.1, 0.3 and 0.5 vol% were used as the test fluid. The results show that the heat transfer of nanofluids is higher than that of the base liquid (water) and increased with the increase in Reynolds number and particle concentrations. The heat transfer rate of nanofluid with 0.5 vol% was 25% greater than that of base liquid, and the results also show that the heat transfer coefficient of the nanofluids at a volume concentration of 0.5 vol% was 15% higher than that of base fluid at given conditions. Pressure drop of nanofluid was increased with increase in volume concentration, and it is slightly higher than that of the base fluid.

**Keywords** Nanoparticle · Nusselt number · Pressure drop · TiO<sub>2</sub>–water nanofluid · Turbulent flow

## List of symbols

$A$	Cross-sectional area (m <sup>2</sup> )	$\rho_p$	Density of nanoparticle (kg m <sup>-3</sup> )
$C$	Specific heat (kJ kg <sup>-1</sup> K <sup>-1</sup> )	$(C_p)_{nf}$	Specific heat of nanofluid (kJ kg <sup>-1</sup> K <sup>-1</sup> )
$D$	Internal diameter of the tube (m)	$(C_p)_f$	Specific heat of base fluid (kJ kg <sup>-1</sup> K <sup>-1</sup> )
$K$	Thermal conductivity (W m <sup>-1</sup> K <sup>-1</sup> )	$(C_p)_p$	Specific heat of nanoparticle (kJ kg <sup>-1</sup> K <sup>-1</sup> )
$T$	Temperature (K)	$K_{nf}$	Thermal conductivity of nanofluid (W m <sup>-1</sup> K <sup>-1</sup> )
$m$	Mass flow rate (kg s <sup>-1</sup> )	$k_p$	Thermal conductivity of nanoparticle (W m <sup>-1</sup> K <sup>-1</sup> )
$Q$	Heat transfer rate (W)	$k_f$	Thermal conductivity of base fluid (W m <sup>-1</sup> K <sup>-1</sup> )
$Nu_{ave}$	Average Nusselt number	$\mu_{nf}$	Dynamic viscosity of nanofluid (kg m <sup>-1</sup> s <sup>-1</sup> )
$h$	Heat transfer coefficient (W m <sup>-1</sup> K <sup>-1</sup> )	$\mu_{bf}$	Dynamic viscosity of base fluid (kg m <sup>-1</sup> s <sup>-1</sup> )
$Re$	Reynolds number	$Q_c$	Heat transfer of cold fluid (kW)
$Nu$	Nusselt number	$Q_h$	Heat transfer of hot fluid (kW)
$g$	Acceleration due to gravity (m s <sup>-2</sup> )	$Q_w$	Heat transfer of base fluid (kW)
$H$	Difference of pressure head (m)	$Q_{nf}$	Heat transfer of nanofluid (kW)
$f$	Friction factor	$Q_{mean}$	Average heat transfer of base fluid and nanofluid (kW)
$L$	Length of the heat exchanger (m)	$T_{ci}$	Temperature of cold fluid inlet (K)
$\rho_{nf}$	Density of nanofluid (kg m <sup>-3</sup> )	$T_{hi}$	Temperature of hot fluid inlet (K)
$\rho_f$	Density of base fluid (kg m <sup>-3</sup> )	$T_{co}$	Temperature of cold fluid outlet (K)
		$T_{ho}$	Temperature of hot fluid outlet (K)
		$h_{nf}$	Convective heat transfer coefficient of nanofluid (kW m <sup>-2</sup> K <sup>-1</sup> )
		$\rho_{cc14}$	Density of carbon tetra chloride (Kg m <sup>-3</sup> )

✉ R. Subramanian  
subramaniannano22@gmail.com

<sup>1</sup> Department of Mechanical Engineering, Sethu Institute of Technology, Pulloor, Kariapatti, Tamilnadu 626115, India

### Greek letters

$\mu$	Dynamic viscosity ( $\text{kg m}^{-1} \text{s}^{-1}$ )
$\varphi$	Volume concentration of nanofluid (%)
$\rho$	Density ( $\text{kg m}^{-3}$ )
$\Delta p$	Pressure drop ( $\text{N m}^{-2}$ )

### Suffix

i	Inner tube or inlet
c	Cold fluid
h	Hot water
f	Base fluid
p	Particle
nf	Nanofluids

## Introduction

Dispersion of nano-sized particles like metals, metal oxides, metal nitrides and carbon based additives in a base fluid is known as nanofluid. These nanofluids are widely used to enhance the heat transfer in boiler cooling systems, heat exchangers, solar collectors, automobile radiators, nuclear flasks and catalytic reactors. Nanofluids offer more possibility to increase heat exchange efficiency than the base fluid. Utilization of nanoparticles with base fluid overcomes most of the problems. Usually nanoparticles were used at very low concentrations; hence, sedimentation in the flow line is very less.

During the past two decades, many of interested researchers have focused their attention to analyze the improvement of thermal conductivity by using nanofluids [1–6]. Many other investigations employed on heat transfer and flow characteristics of nanofluid in double-pipe heat exchanger [7–16]. The convective heat transfer of nanofluids under turbulent flow conditions was analyzed by Pak and Cho [17]. The heat transfer coefficient of nanofluids was 26% more than that of pure water, and the heat transfer coefficient of the nanofluids at about 2% volume concentration was 14% higher compared to that of base fluid–water for the same condition. Freidoonimehr et al. [18] derived the three-dimensional flow models by using nonlinear differential and Navier–Stokes equations for a rotating channel. Ding et al. [19] conducted an experimental study on heat transfer of nanofluids in the condition of laminar flow. Through this study, they proved that the heat transfer coefficient of nanofluid is greater than the pure water and the enhancement also depends on nanoparticle's volume fraction, and the flow conditions. Sarafraz et al. [20] performed forced convection experiments in laminar and turbulent flow regimes. Their results showed that the nanofluid can

enhance the thermal conductivity up to 56% compared to base fluids. Investigation of flow and heat transfer of nanofluids was carried out by Diao et al. [21]. They concluded that the friction factor and Nusselt number of nanofluids are higher than the water. Duangthongsuk and Wongwises [22] studied experimentally on the pressure drop and heat transfer performance of  $\text{TiO}_2$ –water nanofluids under turbulent flow regime and concluded that compared to the base fluid pressure drop is slightly higher for nanofluid in that turbulent regime. The effects of flow rate, Reynolds's number and concentration of nanofluids in concentric tube heat exchanger were studied by Rohit et al. [23]. Their results showed that the average heat transfer rate increased with concentration of nanofluids. Murshed et al. [24] determined the thermal conductivities of  $\text{TiO}_2$ –water nanofluids by using transient hot-wire method, and their result showed that 33% enhancement of thermal conductivity was obtained for the nanofluid with 5% volumetric concentration of nanoparticles.

Recently, heat transfer of nanofluid in laminar forced convection through a bent channel was numerically investigated by Yuan et al. [25]. Then they concluded from this study that the local and average Nusselt number increased with increasing nanoparticle volume fraction. Rashidi et al. [26] and Abbas et al. [27] studied entropy generation on magnetohydrodynamic blood flow of a nanofluid stimulated by peristaltic waves. Then they presented mathematical models for the physical parameters of velocity, concentration, temperature, and entropy. Their numerical computation has been used to assess the pressure rise and friction forces. Natural convection performance of alumina–water nanofluid under the magnetic field was investigated by Makulati et al. [28]. Their results pointed out that the influence of nanofluid on Nusselt number decreases by increasing Hartmann number. Kasaeian et al. [29] analyzed the flow and heat transfer of nanofluid in forced convection. Through this analysis, they concluded that the flow of nanofluid depends on type and volume fraction of nanoparticles and these parameters also increase the value of Nusselt number and heat transfer rate. Karimipour-Fard et al. [30] carried out a numerical study on enhancement of heat transfer and design of heat exchanger. Then they resulted that the cooling rate 40% can be improved by using porous media. Analysis of various thermal properties, heat transfer characteristics and effect of friction factor of hybrid nanofluids was done by Syam Sundar et al. [31]. In this analysis, they observed that thermal conductivity of nanofluids increased with temperature and mass concentration. Naseemaa et al. [32] studied about heat transfer enhancement of heat exchanger by using aluminum oxide, copper oxide nanofluids with different concentrations. Through their study, they observed that  $\text{Al}_2\text{O}_3$  nanoparticles can enhance the convective heat

transfer significantly and it increases with increase in Reynolds number and also with concentration of nanoparticles. The heat transfer and flow characteristics of a hybrid nanofluid was investigated by Phanindra et al. [33] which consists of transformer oil and 0.1% volume concentration of Al<sub>2</sub>O<sub>3</sub>/Cu nanoparticles. In this study, they determined the properties of this nanofluid such as thermal conductivity, density, viscosity. Moradi et al. [34] conducted one experimental investigation on the heat transfer characteristics of nanofluids with multi-walled carbon nanotube in a countercurrent double-pipe heat exchanger. From this study, they concluded that the highest increment (35%) was obtained in the heat transfer coefficient, at the lowest mass fraction (0.04 mass%) within the experiment range.

With the above detailed discussion about previous studies, most of the researchers reported about the heat transfer performance and pressure drop in double-pipe heat exchanger by using nanofluids under laminar or turbulent regime alone. However, very minimum scholars studied about heat transfer performance of nanofluids in transition flow regime. Intention of this present experimental study is to analyze the effect of TiO<sub>2</sub>-water nanofluid on heat transfer enhancement with various flow regimes of laminar, transition and turbulent with different volume concentrations like 0.1%, 0.3% and 0.5%. The effect of volume concentration of nanoparticles on various performance parameters is discussed and demonstrated in detail.

## Experimentation

Experimental process consists of two important activities. First one is nanofluid preparation, and second one is fabrication of experimental setup and conducting experiments. Both are discussed in the following chapters.

### Preparation of nanofluid

To conducting this experiment, nanofluid preparation is the first step. For this study, the nanofluids with volume concentrations of 0.1 vol%, 0.3 vol%, and 0.5 vol% were prepared at Nano Laboratory of National Institute of Technology, Tiruchirappalli, India, by dispersing TiO<sub>2</sub> nanoparticles with an average size of 20 nm in de-ionized water. For accurate experimental results, the nanofluid should be homogeneous, steady and none of the sedimentation. Hence, the prepared TiO<sub>2</sub>-water nanofluids were kept under ultrasonication process for 4–5 h to obtain the uniform dispersion of nanoparticles. Following this, the sonicated nanofluids were stirred continuously for 2 h. Then, the TiO<sub>2</sub> nanofluids are kept stationary for

observation and found that no particle settlement at the bottom of the flask even after 48 h.

## Experimental setup

For this analysis, the experimental setup was fabricated with the following equipments, (a) double-pipe counter-flow heat exchanger, (b) nanofluid and hot water circulation units, (c) heating unit for working fluid, (d) temperature measurement units, (e) flow measuring equipments. Figure 1 shows the schematic diagram of double-pipe counter-flow heat exchanger, and Fig. 2 shows photographic view of experimental setup.

Test section of double-pipe counter-flow heat exchanger is provided with length of 885 mm. The inner copper tube has inner diameter of 7 mm and outer diameter of 10 mm and total length of 3000 mm. The outer tube made of GI with inner diameter of 22 mm and outer diameters of 27.5 mm. Table 1 shows the specification of double-pipe counter-flow heat exchanger test section.

Nanofluid circulation system consists of the following items: (a) reservoir/collection tank, (b) pump with bypass line, (c) rotameter, (d) heat transfer test section, and (e) radiator. From the reservoir, pump is used to circulate the nanofluid throughout the circuit. Required mass flow rate of the nanofluid is obtained by the adjustment of return valve and rotameter. The radiator is used to control the temperature of nanofluid and keep it constant at the inlet of the test section.

Hot water circulation system consists of the following items: (a) reservoir/collection tank, (b) pump with bypass line, (c) rotameter, and (d) heat transfer test section. In reservoir tank, 1500 W electric heater was installed with thermostat which is used to maintain the temperature of hot water. Hot water pumped from the reservoir tank and circulates it throughout the circuit. The required mass flow rate of the hot water is obtained by the adjustment of return valve and rotameter.

Seven thermocouples were connected in the test section. Four k-type thermocouples are used to measure the inlet and outlet temperature of nanofluid and hot water. Three k-type thermocouples are installed at test section at a distance of 240 mm, 420 mm and 600 mm from the left end, respectively. Test section was isolated by a 10 mm thickness with insulation material in order to minimize the heat loss to the surroundings.

A CCl<sub>4</sub> manometer was used to measure the pressure drop. The pressure drop was calculated from the change in the height of manometer column.

The mass flow rate of the hot water (333 k) was maintained as 5 lpm (L/min) for all experimental trials. For each and every test, the hot water inlet, outlet, nanofluid inlet, outlet and intermediate wall temperatures were recorded.

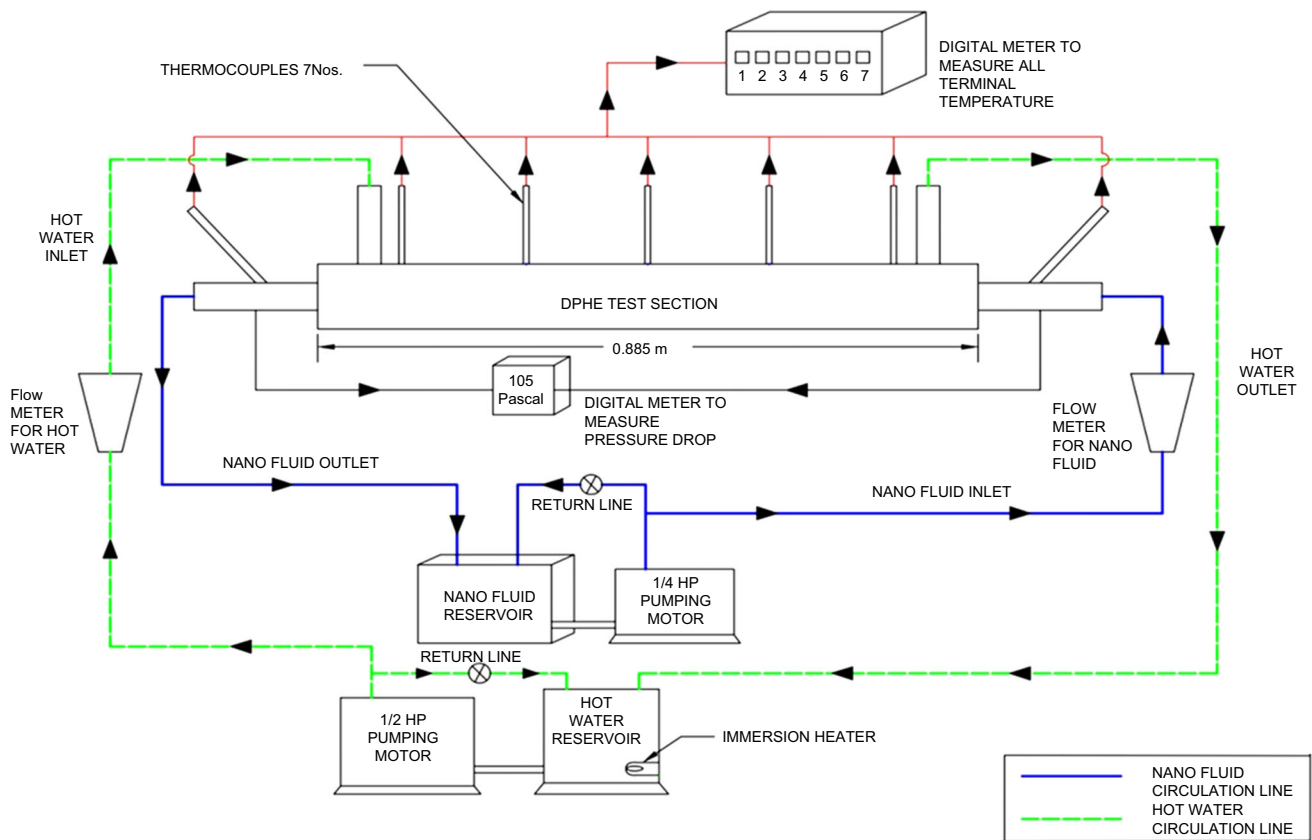


Fig. 1 Schematic diagram of double-pipe counter-flow heat exchanger

Fig. 2 Photographic view of experimental setup



Table 1 Specification of test section

Part name	Material	Inner diameter in mm	Thickness in mm	Length in mm
Inner tube	Copper	7	1.5	885
Outer pipe	GI	22	2.75	885

For various flow rates such as 0.2 lpm, 0.4 lpm, 0.6 lpm and 0.8 lpm, pressure drop readings were noted after the steady state was reached. Sufficient pipe length is provided before the fluid entering into the test section. Hence, the flow is thermally and hydro-dynamically fully developed one.

Adequate experiments with hot and cold water have been carried out with the same input parameters. An average is taken into consideration. It was found that the deviation is within 5%. Nusselt numbers obtained from standard correlations were compared with experimental values for assessing the consistency. The result shows good agreement and within the limit.

### Uncertainty analyses

The uncertainties in the measurements are defined as the root sum square of the fixed error of the instrument and random error observed during various measurements. The characteristics of the various measuring instruments used in the experiments are given in Table 2.

Uncertainties associated with the dependent variables like Reynolds number, friction factor and Nusselt number are also estimated using the following equations [35]. Uncertainty in a measurement consists of two major components such as bias error and random error. Bias error is a constant and systematic error in the process. Random error is the repeatability error. The uncertainty in the experimental measurements is defined as the root mean square of the fixed error and the random error.

$$\text{Uncertainty} = \sqrt{(B^2 + R_E^2)} \tag{1}$$

$$\frac{\Delta Re}{Re} = \left[ \left( \frac{\Delta m}{m} \right)^2 + \left( \frac{\Delta d}{d} \right)^2 \right]^{0.5} \tag{2}$$

$$\frac{\Delta f}{f} = \left[ \left( \frac{\Delta(\Delta p)}{\Delta p} \right)^2 + \left( \frac{\Delta L}{L} \right)^2 + \left( 3 \frac{\Delta d}{d} \right)^2 + \left( 2 \frac{\Delta Re}{Re} \right)^2 \right]^{0.5} \tag{3}$$

$$\frac{\Delta Nu}{Nu} = \left[ \left( \frac{\Delta V}{V} \right)^2 + \left( \frac{\Delta I}{I} \right)^2 + \left( \frac{\Delta d}{d} \right)^2 + \left( \frac{\Delta T_s}{T_s} \right)^2 + \left( \frac{\Delta T_b}{T_b} \right)^2 \right]^{0.5} \tag{4}$$

The calculations pointed out that the uncertainties involved are ± 0.5% for Reynolds number, ± 1.4% for friction factor and ± 0.14% for Nusselt number. The experimental results are reproducible within these uncertainty ranges.

### Data reduction

The experimental data were used to calculate the Reynolds number, heat transfer rate, heat transfer coefficient, Nusselt number of Nanofluids with various percentages of volume concentrations.

### Properties of nanofluid

The thermophysical properties of nanofluids used in this study were obtained by using the following equations.

#### Density of nanofluid

The density of the nanofluid was calculated by the use of the Pak and Cho [17] correlation, which was defined as follows.

$$\rho_{nf} = \phi \rho_p + (1 - \phi) \rho_f \tag{5}$$

#### Specific heat of the nanofluid

C<sub>pnf</sub> is the effective specific heat of the nanofluids which can be calculated from Xuan and Roetzel relation [36] which is given as:

$$C_{pnf} = \left[ \frac{\left( \phi (\rho C_p)_p + (1 - \phi) (\rho C_p)_f \right)}{\rho_{nf}} \right] \tag{6}$$

**Table 2** Accuracies and ranges of measuring instruments

Instrument	Range	Accuracy	Uncertainty/%
Temperature indicator	0–500 °C	± 1 °C	3.3
Manometer	500 mm	1 mm	4
Rotameter	0–10 LPM (hot water)	0.2 LPM	± 2
	0–1 LPM (nanofluid)	0.02 LPM	± 2
Ammeter	0–20 Amps	0.01 amp	0.2
Voltmeter	0–220 Volts	0.1 V	0.2

### Thermal conductivity of the nanofluid

Thermal conductivity of the nanofluids can be evaluated by Maxwell correlations given as follows [36]:

$$K_{nf} = K_f \left[ \frac{K_p + 2K_f - 2\phi(K_f - K_p)}{K_p + 2K_f + \phi(K_f - K_p)} \right] \quad (7)$$

Maxwell's formula shows the effective thermal conductivity of nanofluids ( $K_{nf}$ ) on the thermal conductivity of spherical particles  $K_p$ , the thermal conductivity of base fluid ( $k_f$ ) and volume concentration of the solid particles ( $\phi$ )

### Viscosity of the nanofluid

In the case of nanofluid

$\mu_i = \mu_{nf}$  = dynamic viscosity of the nanofluid can be evaluated by the correlations given by Brinkman [37] extended Einstein's formula to be used with moderate particle concentrations. For particle concentrations less than 4%, the expression is as follows:

$$\mu_{nf} = \mu_{bf}(1 - \phi)^{2.5} \quad (8)$$

### Heat transfer between hot water and nanofluid

Heat gained by the cold Water is given as [38]

$$Q_c = m_c C_c (T_{co} - T_{ci}) \quad (9)$$

Heat lost by the hot water is given as [39]

$$Q_h = m_h C_h (T_{hi} - T_{ho}) \quad (10)$$

Heat gained by the cold fluid (with TiO<sub>2</sub>-water nanofluid) is given as [38]

$$Q_{nf} = m_{nf} C_{nf} (T_{out} - T_{in}) \quad (11)$$

$$Q_{mean} = \left( \frac{Q_{water} + Q_{nf}}{2} \right) \quad (12)$$

The convective heat transfer coefficient for nanofluid was calculated from the following equation: [40, 41]

$$h_{nf} = \left( \frac{Q_{mean}}{A(T_{wall} - T_{nfin})} \right) \quad (13)$$

The Nusselt number for nanofluid was calculated from the following equation [35]

$$Nu_{nf} = \left( \frac{h_{nf} D}{K_{nf}} \right) \quad (14)$$

Reynolds number can be calculated by (Re) [35]

$$Re = \left( \frac{d_i m_i}{\mu_i a_i} \right) \quad (15)$$

The pressure drop may be calculated ( $\Delta P$ ) [35]

$$\Delta p = H(\rho_{ccl4} - \rho_w) \quad (16)$$

The friction factor can be calculated for laminar flow as ( $f$ ) [35]

$$f = \left( \frac{64}{Re} \right) \quad (17)$$

### Theoretical Nusselt number

Nusselt number is calculated from Duangthongsuk and Wong wiset correlation [22] as follows:

$$Nu = 0.074 Re^{0.707} Pr^{0.38} \phi^{0.074} \quad (18)$$

## Result and discussion

### Effect of volume concentration

The presence of TiO<sub>2</sub> nanoparticles enhances the thermal conductivity of base fluid-water due to particle migration, disordered movement and the mixing effect of particle near the wall leading to the increase in heat transfer rate. An enhancement in heat transfer rate is observed due to the addition of nanoparticles even at very low concentrations. 5.4% increase in heat transfer rate is observed for a lower Nanofluid concentration, and for 0.5 vol% of TiO<sub>2</sub> nanofluid, a further increase in the heat transfer rate of 25% is observed. The relation between Reynolds number and heat transfer rate is shown in Fig. 3. Heat transfer rate increased with increase in Reynolds number. The same trend is

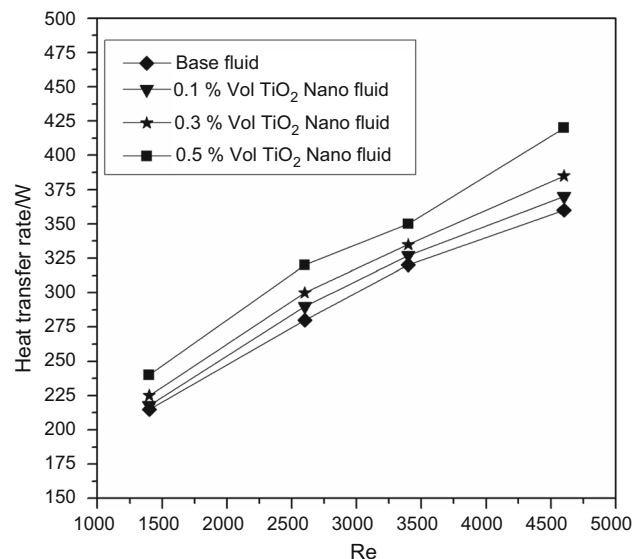


Fig. 3 Variation of heat transfer rate with Reynolds number

followed in many of previous experiments [1, 12, 13]. When comparing the heat transfer rate in three different flow patterns, the slope of heat transfer rate in transition region is slightly higher compared to other two flow patterns.

**Effect of Reynolds number on pressure drop**

Relationship between Reynolds numbers on pressure drop for base fluid and nanofluids with various concentrations is shown in Fig. 4. The experimental results showed the pressure drop of 26%, 35% and 56% higher than the base fluid for 0.1 vol%, 0.3 vol% and 0.5 vol% of TiO<sub>2</sub> nanofluid in laminar flow regime.

When comparing the experimental result of conventional heat transfer, heat transfer in transition flow showed that average enhancement of pressure drop is 34%, 40% and 60% for 0.1 vol%, 0.3 vol% and 0.5 vol% of TiO<sub>2</sub> nanofluid.

When comparing the experimental result of conventional heat transfer V<sub>S</sub> nanofluid heat transfer of turbulent flow, it showed that average increment of pressure drop is 37%, 42% and 62% for 0.1 vol%, 0.3 vol% and 0.5 vol% of TiO<sub>2</sub> nanofluid.

**Effect of Reynolds number on friction factor**

Figure 5 shows the variation of friction factor with respect to Reynolds number. When comparing experimental results in laminar flow, it showed that the average enhancement of friction factor is 38%, 45% and 64% for 0.1 vol%, 0.3 vol% and 0.5 vol% of TiO<sub>2</sub> nanofluids.

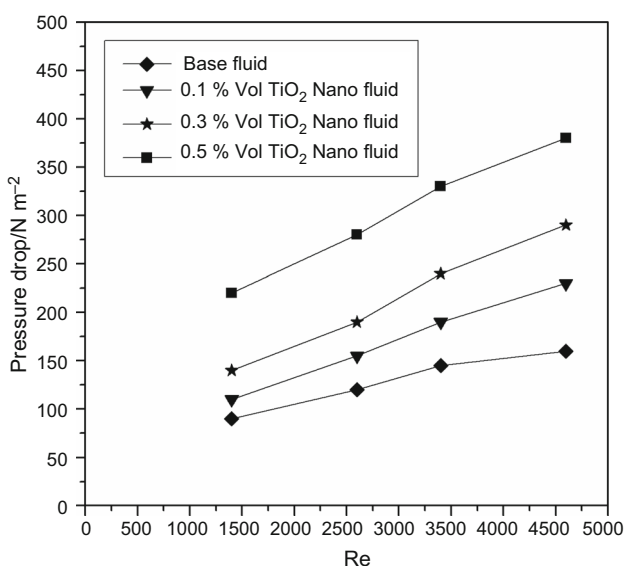


Fig. 4 Variation of pressure drop with Reynolds number

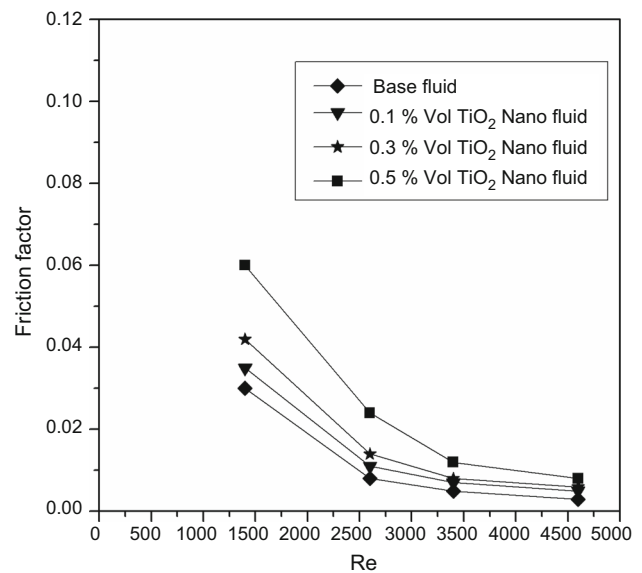


Fig. 5 Variation of friction factor with Reynolds number

When comparing experimental results in transition flow, it showed that the enhancement of friction factor is 42%, 47% and 66% for 0.1 vol%, 0.3 vol% and 0.5 vol% of TiO<sub>2</sub> nanofluids. In turbulent flow, it showed that the increase in friction factor is 44%, 50% and 63% for 0.1 vol%, 0.3 vol% and 0.5 vol% of TiO<sub>2</sub> nanofluid.

The increase in volume concentration increases the friction factor. It was because the increase in TiO<sub>2</sub> nanoparticles increases the viscosity of base fluid accompanied by the increase in heat transfer enhancement. Experimental result showed that the friction factor is more when the flow is laminar and it is normal when it is transition and the friction factor decreases when the flow is turbulent and when the mass flow rate is increasing.

**Effect of Reynolds number on Nusselt number**

Figure 6 shows the effect of TiO<sub>2</sub> water nanofluids on the Nusselt number with reference of Reynolds number. The addition of nanoparticles augments the overall thermal storage capacity and augments the effective dynamic viscosity which has adverse impact on convection. The increase in volume concentration increases the Nusselt number. It was due to the increase in thermal conductivity of water.

The highest Nusselt number reached at 0.5% of volume concentration. When the volume concentration increases, simultaneously the surface area of the particle also increases and enhances the heat transfer rate leading to the increase in Nusselt number.

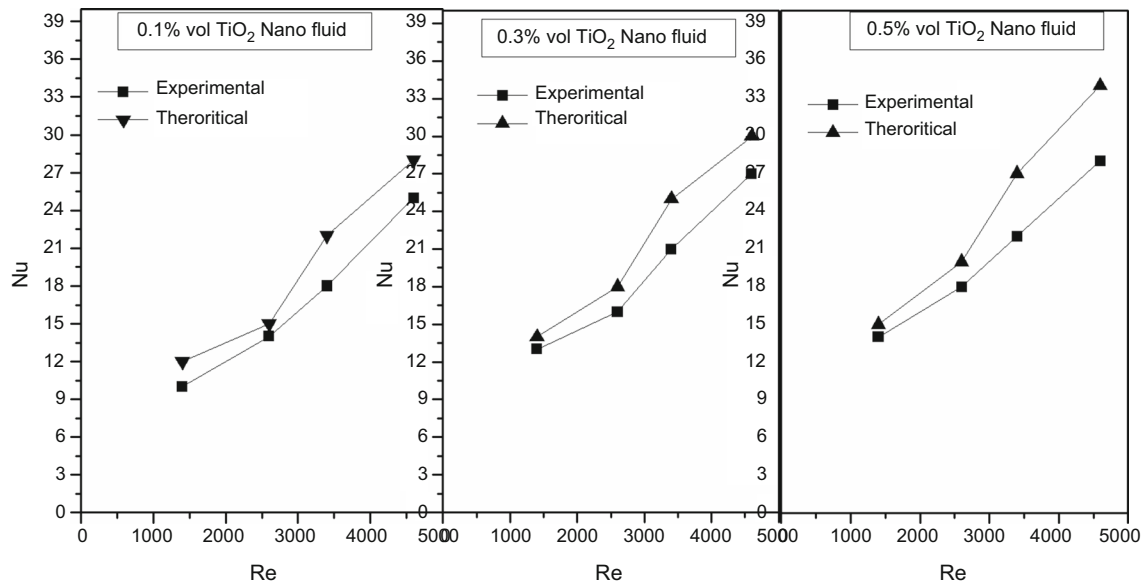


Fig. 6 Variation of Nusselt number with Reynolds number

**Performance evaluation criteria**

Performance evaluation criteria (PEC) [8] are calculated from the following formula

$$PEC = \left[ \frac{Nu_{nanofluid}}{Nu_{basefluid}} \left( \frac{f_{nanofluid}}{f_{basefluid}} \right)^{1/3} \right] \tag{19}$$

In base or nanofluid, PEC is minimum at low flow rate and maximum at high flow rate. That is PEC increased with Reynolds number which is presented in Fig. 7. In

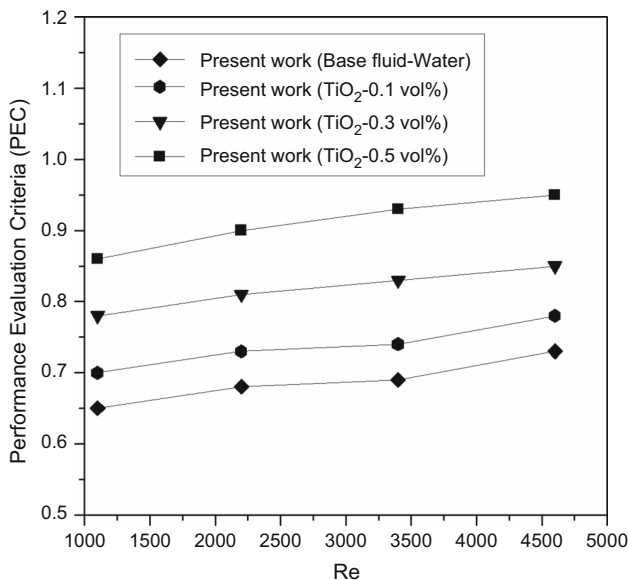


Fig. 7 Variation of performance evaluation criteria (PEC) with Reynolds number

nanofluid, PEC is also increased with percentage of volume concentration.

**Correlation equation**

In this present work, a new correlation equation (Equation no. 20) was derived from the data obtained from the tests with various volume fractions of nanofluids. It is a function of Reynolds number, and volume fraction of nanoparticles is as follow:

$$Nu = 0.44Re^{0.465} \varphi^{-0.052} \tag{20}$$

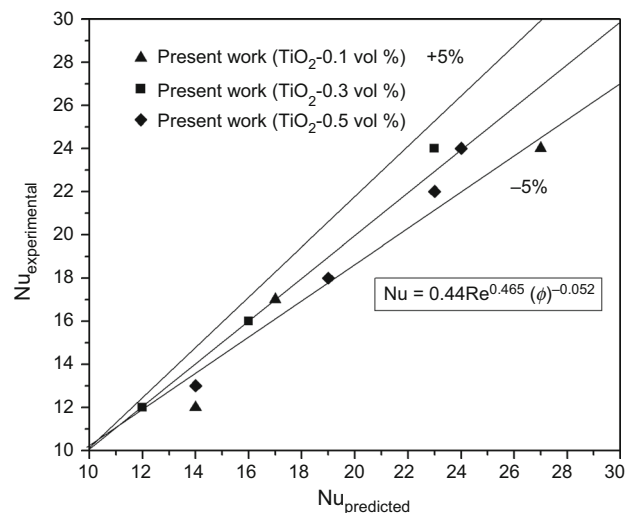
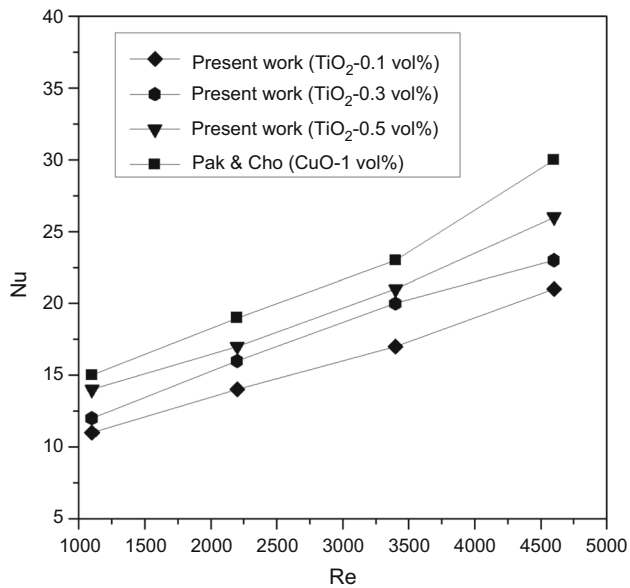


Fig. 8 Relation between experimental and correlated values of Nusselt numbers





**Fig. 9** Comparison with previous work—effect of Nusselt number with Reynolds number

The predicted Nusselt number values within  $\pm 5\%$  in comparison with those with experimental data. Figure 8 shows the relation between experimental data and correlated values of Nusselt numbers.

In this work, for 0.1 vol% of TiO<sub>2</sub> nanofluid, the Nusselt number increases from 11 to 20. For 0.3 vol% of TiO<sub>2</sub> nanofluid, the Nusselt number increases from 12 to 23. For 0.5 vol% of TiO<sub>2</sub> nanofluid, the Nusselt number increases from 14 to 25. It shows that whenever the flow rate increases, the Nusselt number increased with Reynolds number as like as previous analysis done by Pak and Cho [17] and it is presented in Fig. 9.

## Conclusions

From the detailed analysis, the following conclusions were obtained. Experimental results showed that the heat transfer enhancement of 5.4%, 14% and 25% for the nanofluid with 0.1 vol%, 0.3 vol% and 0.5 vol% of TiO<sub>2</sub> nanoparticles. It shows that the enhancement of heat transfer is directly proportional to volume concentration of nanofluid and mass flow rate of the nanofluid. The nanoparticles increase the surface area which results in increase in the heat transfer rate. Experimental result showed that the pressure drop is directly proportional to the mass flow rate and concentration of the TiO<sub>2</sub> nanoparticles. Based on flow, pressure drop is directly proportional to Reynolds Number. By the use of nanofluid, the heat transfer rate is increased considerably which leads to the reduction in the size of the heat exchanger and in the fabrication cost. In

future it is expected that nanofluid can make substantial impact in heat exchangers.

## References

- Duangthongsuk W, Wongwises S. Heat transfer enhancement and pressure drop characteristics of TiO<sub>2</sub>-water nanofluid in a double-tube counter flow heat exchanger. *Int J Heat Mass Transf.* 2009;52(7):2059–67. <https://doi.org/10.1016/j.ijheatmasstransfer.2008.10.023>.
- Arabpour A, Karimipour A, Toghraie D. The study of heat transfer and laminar flow of kerosene/multi-walled carbon nanotubes (MWCNTs) nanofluid in the microchannel heat sink with slip boundary condition. *J Therm Anal Calorim.* 2018;131(2):1553–66. <https://doi.org/10.1007/s10973-017-6649-x>.
- Hemmat EM, Hassani AMR, Toghraie D, Hajmohammad MH, Rostamian H, Tourang H. Designing artificial neural network on thermal conductivity of Al<sub>2</sub>O<sub>3</sub>-water-EG (60–40%) nanofluid using experimental data. *J Therm Anal Calorim.* 2016;126:837–43.
- Afshari A, Akbari M, Toghraie D, Yazdi ME. Experimental investigation of rheological behavior of the hybrid nanofluid of MWCNT-alumina/water (80%)-ethylene-glycol (20%). *J Therm Anal Calorim.* 2018;132(2):1001–15. <https://doi.org/10.1007/s10973-018-7009-1>.
- Mahian O, Kolsi L, Amani M, Estellé P, Ahmadi G, Kleinstreuer C, Marshall JS, Siavashi M, Taylor RA, Niazmand H, Wongwises S, Hayat T, Kolanjiyil A, Kasaeian A, Pop I. Recent advances in modeling and simulation of nanofluid flows—part I: fundamentals and theory. *Phys Rep.* 2018. <https://doi.org/10.1016/j.physrep.2018.11.004>.
- Esfahani NN, Toghraie D, Afrand M. A new correlation for predicting the thermal conductivity of ZnO-Ag (50%–50%)/water hybrid nanofluid: an experimental study. *Powder Technol.* 2018;323:367–73.
- Chun BH, Kang HU, Hyun KS. Effect of alumina nanoparticles in the fluid on heat transfer in double pipe heat exchanger system. *Korean J Chem Eng.* 2008;25:966–71. <https://doi.org/10.1007/s11814-008-0156-5>.
- Muthusamy V, Skryabin S. Effect of conical cut-out turbulators with internal fins in a circular tube on heat transfer and friction factor. *Int Commun Heat Mass Transf.* 2013;44:64–8. <https://doi.org/10.1016/j.icheatmasstransfer.2013.03.004>.
- Zadkhast M, Toghraie D, Karimipour A. Developing a new correlation to estimate the thermal conductivity of MWCNT-CuO/water hybrid nanofluid via an experimental investigation. *J Therm Anal Calorim.* 2017;129(2):859–67. <https://doi.org/10.1007/s10973-017-6213-8>.
- Rabienataj DA, Farhadi M, Sedighi K. Heat transfer and flow characteristics of Al<sub>2</sub>O<sub>3</sub>-water nanofluid in a double tube heat exchanger. *Int Commun Heat Mass Transf.* 2013;47:105–12. <https://doi.org/10.1016/j.icheatmasstransfer.2013.06.003>.
- Aghayari R, Maddah H, Ashori F, Hakiminejad A, Aghili M. Effect of nanoparticles on heat transfer in mini double pipe heat exchangers in turbulent flow. *Heat Mass Transf.* 2013. <https://doi.org/10.1007/s00231-014-1415-0>.
- Reddy MCS, Rao VV. Experimental investigation of heat transfer coefficient and friction factor of ethylene glycol water based TiO<sub>2</sub> nanofluid in double pipe heat exchanger with and without helical coil inserts. *Int Commun Heat Mass Transf.* 2014;50:68–76. <https://doi.org/10.1016/j.icheatmasstransfer.2013.11.002>.

13. Khedkar R, Sonawane SS, Wasewar KL. Heat transfer study on concentric tube heat exchanger using  $\text{TiO}_2$ -water-based nanofluid. *Int Commun Heat Mass Transf*. 2014. <https://doi.org/10.1016/j.icheatmasstransfer.2014.07.011>.
14. Muthusamy C, Gowtham M, Manickam S, Manjunathan M, Srithar K. Enhancement of productivity of humidification–dehumidification desalination using modified air heater. *Desalination Water Treat*. 2015;56(12):3294–304. <https://doi.org/10.1080/19443994.2014.968876>.
15. Esfe MH, Hajmohammad H, Toghraie D, Rostamian H, Mahian O, Wongwises S. Multi-objective optimization of nanofluid flow in double tube heat exchangers for applications in energy systems. *Energy*. 2017;137:160–71. <https://doi.org/10.1016/j.energy.2017.06.104>.
16. Hosseini-zhad R, Akbari OA, Afrouzi HH, Biglarian M, Koveiti A, Toghraie D. Numerical study of turbulent nanofluid heat transfer in a tubular heat exchanger with twin twisted-tape inserts. *J Therm Anal Calorim*. 2018;132(1):741–59. <https://doi.org/10.1007/s10973-017-6900-5>.
17. Pak BC, Cho YI. Hydrodynamic and heat transfer study of dispersed fluids with submicron metallic oxide particles. *Exp Heat Transf*. 1998;11:151–70.
18. Freidoonimehr N, Rostami B, Rashidi MM, Omoniat E. Analytical modelling of three-dimensional squeezing nanofluid flow in a rotating channel on a lower stretching porous wall., *Mathematical Problems in Engineering* London: Hindawi Publishing Corporation; 2014. p. 1–14. <https://doi.org/10.1155/2014/692728>.
19. Ding Y, Alias H, Wen D, Williams RA. Heat transfer of aqueous suspensions of carbon nanotubes (CNT nanofluids). *Int J Heat Mass Transf*. 2005;49:240–50. <https://doi.org/10.1016/j.ijheatmasstransfer.2005.07.009>.
20. Sarafraz MM, Hormozi F, Nikkha V. Thermal performance of a counter-current double pipe heat exchanger working with COOH-CNT/water nanofluids. *Exp Therm Fluid Sci*. 2016;78:41–9. <https://doi.org/10.1016/j.expthermflusci.2016.05.014>.
21. Diao Y, Li CZ, Zhang J, Zhao Y, Kang Y. Experimental investigation of MWCNT-water nanofluids flow and convective heat transfer characteristics in multiport minichannels with smooth/micro-fin surface. *Powder Technol*. 2017;305:206–16. <https://doi.org/10.1016/j.powtec.2016.10.011>.
22. Duangthongsuk W, Wongwises S. An experimental study on the heat transfer performance and pressure drop of  $\text{TiO}_2$ -water nanofluids flowing under a turbulent flow regime. *Int J Heat Mass Transf*. 2010;53(1–3):334–44. <https://doi.org/10.1016/j.ijheatmasstransfer.09.024>.
23. Rohit K, Shriram S, Kailas W. Heat transfer study on concentric tube heat exchanger using  $\text{TiO}_2$ -water-based nanofluids. *Int Commun Heat Mass Transf*. 2014;57:163–9.
24. Murshed SMS, Leong KC, Yang C. Enhanced thermal conductivity of  $\text{TiO}_2$ -water based nanofluids. *Int J Therm Sci*. 2005;44(4):363–73. <https://doi.org/10.1016/j.ijthermalsci.2004.12.005>.
25. Ma Y, Mohebbi R, Rashidi ZY. Study of nanofluid forced convection heat transfer in a bent channel by means of lattice Boltzmann method. *Phys Fluids*. 2018;30:032001–13. <https://doi.org/10.1063/1.5022060>.
26. Rashidi MM, Bhatti MM, Abbas MA, Ali ME-S. Entropy generation on MHD blood flow of nanofluid due to peristaltic waves. *Entropy*. 2016;18(117):1–16. <https://doi.org/10.3390/e18040117>.
27. Ali Abbas M, Bai YQ, Rashidi MM, Bhatti MM. Application of drug delivery in magnetohydrodynamics peristaltic blood flow of nanofluid in a non-uniform channel. *J Mech Med Biol*. 2016;16(4). <https://doi.org/10.1142/S0219519416500524>.
28. Makulati N, Kasaeipoor A, Rashidi MM. Numerical study of natural convection of a water–alumina nanofluid in inclined C-shaped enclosures under the effect of magnetic field. *Adv Powder Technol*. 2016;27(2):661–72. <https://doi.org/10.1016/j.apt.2016.02.020>.
29. Kasaeian A, Daneshzarian R, Mahian O, Kolsi L, Chamkha A, Wongwises S, Pop I. Nanofluid flow and heat transfer in porous media: a review of the latest developments. *Heat Mass Transf*. 2017;107:778–91. <https://doi.org/10.1016/j.ijheatmasstransfer.2016.11.074>.
30. Karimipour-Fard P, Afshari E, Ziaei-Rad M, Taghian-Dehghani S. A numerical study on heat transfer enhancement and design of a heat exchanger with porous media in continuous hydrothermal flow synthesis system. *Chin J Chem Eng*. 2017. <https://doi.org/10.1016/j.cjche.2017.01.015>.
31. Syam Sundar L, Sharma KV, Singh MK, Sousa ACM. Hybrid nanofluids preparation, thermal properties, heat transfer and friction factor—a review. *Renew Sustain Energy Rev*. 2017. <https://doi.org/10.1016/j.rser.2016.09.108>.
32. Naseema SK, NawazishMehdia S, Hussain MM, Basha SK, Samad MA. Heat enhancement of heat exchanger using aluminium oxide ( $\text{Al}_2\text{O}_3$ ), copper oxide (CUO) nanofluids with different concentrations. *Mater Today Proc*. 2018;5(2):6481–8. <https://doi.org/10.1016/j.matpr.2017.12.261>
33. Phanindra Y, Kumar SD, Pugazhendhi S. Experimental investigation on  $\text{Al}_2\text{O}_3$  & Cu/Oil hybrid nano fluid using concentric tube heat exchanger. *Mater Today Proc*. 2018;5(2):12142–50. <https://doi.org/10.1016/j.matpr.2018.02.192>.
34. Moradi A, Toghraie D, Isfahani AHM, Hosseini A. An experimental study on MWCNT-water nanofluids flow and heat transfer in double-pipe heat exchanger using porous media. *J Therm Anal Calorim*. 2019;1:21. <https://doi.org/10.1007/s10973-019-08076-0>.
35. Suresh S, Chandrasekar M, Chandrasekhar S. Experimental studies on heat transfer and friction factor characteristics of CuO/water nanofluid under turbulent flow in a helically dimpled tube. *Exp Therm Fluid Sci*. 2011;35:542–9.
36. Xuan Y, Roetzel W. Conceptions for heat transfer correlations of nanofluids. *Int J Heat Mass Transf*. 2000;43:3701–7.
37. Brinkman H. The viscosity of concentrated suspensions and solutions. *J Chem Phys*. 1952;20:571–82.
38. Kakac S, Liu H. Heat exchangers: selection, rating, and thermal design. 2nd ed. CRC Press; 2002. p. 131–227.
39. Swamee PK, Aggarwal N. Optimum design of double pipe heat exchanger. *Int J Heat Mass Transf*. 2008;51:2260–6.
40. Bell KJ. Final report of the cooperative research program on shell and tube heat exchangers. Engineering Experiment Station Bulletin. University of Delaware; 1963.
41. Rohsenow WM, Hartnett JR, Cho YI. Chapter 5: Forced convection, internal flow in ducts. In: *Handbook of Heat Transfer*. 3rd ed. New York: McGraw-Hill; 1944.

**Publisher's Note** Springer Nature remains neutral with regard to jurisdictional claims in published maps and institutional affiliations.